Original Paper

Perfusion

Perfusion
2014, Vol. 29(4) 340–350

DOI: 10.1177/0267659114521103
prf.sagepub.com
SAGE

Combining numerical and clinical methods to assess aortic valve hemodynamics during exercise

HG Bahraseman,[1] K Hassani,[1] A Khosravi,[2] M Navidbakhsh,[3] DM Espino,[4] N Fatouraee[5] and D Kazemi-Saleh[2]

Abstract

Computational simulations have the potential to aid understanding of cardiovascular hemodynamics under physiological conditions, including exercise. Therefore, blood hemodynamic parameters during different heart rates, rest and exercise have been investigated, using a numerical method. A model was developed for a healthy subject. Using geometrical data acquired by echo-Doppler, a two-dimensional model of the chamber of aortic sinus valsalva and aortic root was created. Systolic ventricular and aortic pressures were applied as boundary conditions computationally. These pressures were the initial physical conditions applied to the model to predict valve deformation and changes in hemodynamics. They were the clinically measured brachial pressures plus differences between brachial, central and left ventricular pressures. Echocardiographic imaging was also used to acquire different ejection times, necessary for pressure waveform equations of blood flow during exercise. A fluid-structure interaction simulation was performed, using an arbitrary Lagrangian-Eulerian mesh. During exercise, peak vorticity increased by 14.8%, peak shear rate by 15.8%, peak cell Reynolds number by 20%, peak leaflet tip velocity increased by 47% and the blood velocity increased by 3% through the leaflets, whereas full opening time decreased by 11%. Our results show that numerical methods can be combined with clinical measurements to provide good estimates of patient-specific hemodynamics at different heart rates.

Keywords

echo-Doppler flow; fluid-structure interaction; hemodynamics; natural aortic valve

Introduction

Cardiovascular disease is a major cause of mortality.[1] Understanding changes to blood flow during exercise is a key element in cardiovascular diagnosis.[2–5] For instance, exercise may be used to evaluate patients with coronary artery disease.[6] Current invasive/non-invasive methods used to assess cardiovascular performance have several limitations, such as being difficult and expensive to use and not being risk free.[7] Computational methods could, instead, be combined with exercise measurements to determine hemodynamics, reducing the need for invasive procedures.

Computational methods have the potential to predict hemodynamics, provided the correct boundary conditions are applied.[6,8–12] Fluid-Structure Interaction (FSI) simulations are well suited to heart valve modeling, such as the aortic valve.[13–18] Fluid flow around a valve causes its deflection and deformation which, in turn, alters fluid flow. In the aortic valve, recirculation in the sinuses of the valsava during left ventricular systole, for example, are known to regulate valve opening and prepare it for closure.[19] Such recirculation is dependent on the deformation of the valve cusps.[20] FSI simulations combine

[1]Department of Biomechanics, Science and Research Branch, Islamic Azad University, Tehran, Iran
[2]Atherosclerosis Research Center, Baqiyatallah University of Medical Sciences, Tehran, Iran.
[3]Department of Mechanical Engineering, Iran University of Science and Technology, Tehran, Iran
[4]School of Mechanical Engineering, University of Birmingham, UK
[5]Department of Biomedical Engineering, Amirkabir University, Tehran, Iran

Corresponding author:
Arezoo Khosravi
Atherosclerosis Research Center
Baqiyatallah University of Medical Sciences
Tehran
Iran.
Email: arekhosravi@yahoo.com

finite element analysis (FEA) of a structure (e.g. the valve cusps) with computational fluid dynamics (CFD) to assess flow (e.g. blood around cusps). FSI requires the use of an arbitrary Lagrange-Euler (ALE) mesh to analyze FEA and CFD.[21] A simultaneous FSI simulation is possible by applying shared constraints at boundaries shared by the fluid and the structure.[22,23]

Computational models developed require validation, which has been performed for several aortic valve FSI models.[13,14,24,25] However, few models combine a numerical simulation with non-invasive clinical measurements to predict a patient's hemodynamics. Recently, we developed and validated a two-dimensional aortic valve FSI model to predict changes to cardiac output and stroke volume caused by changes in heart rate during exercise.[26] The variation of flow patterns across the aortic valve, including variation of vorticity, shear rate, stress and strain on the leaflets during exercise, were not reported. However, given the large changes in stroke volume and cardiac output, large transient changes to flow-patterns across the aortic valve are anticipated with exercise and heart rate.

Therefore, the aim of this study was to determine the effect of exercise on blood flow hemodynamics. Our existing two-dimensional aortic valve FSI model has been used to assess changes to blood flow during exercise. The boundary conditions and key valve dimensions for our model were obtained from a single volunteer, making our predictions subject specific. Blood flow parameters assessed include: vorticity, shear rate, blood velocity through the aortic orifice region, local cell Reynolds, leaflet tip velocity; time to full opening, full opening duration and time to closure contact.

Methods

Overview

We have described and validated our subject-specific two-dimensional FSI model in depth previously [3]. Here, a brief overview is provided of the model and clinical measurements (combined clinical and numerical approach). The Analysis of fluid dynamics section below details the fluid dynamics measurements investigated in this present study.

Combined clinical and numerical approach

A healthy male, aged 33 years, participated in this study with his hemodynamic data recorded during rest and exercise. Informed consent was obtained for the participant, according to protocols approved by the Department of Cardiovascular Imaging (Shaheed Rajaei Cardiovascular, Medical and Research Center, Tehran, Iran). Following physical examination, the volunteer was found to have normal cardiovascular performance. This was determined from maximal bicycle exercise tests and Doppler ECG. Systolic and diastolic pressures of the brachial artery were measured and related to heart rate changes at rest and exercise (Figure 1). Equations 1 and 2 were used to determine the central pressure from brachial pressure measurements. This relationship was previously determined by comparing brachial pressure (acquired by oscillometry) to the central pressure acquired using an invasive method [43].

$$\textit{Central diastolic pressure} \approx \textit{Brachial diastolic pressure} + 2.25 \quad (1)$$

$$\textit{Central diastolic pressure} \approx \textit{Brachial diastolic pressure} - 5.45 \quad (2)$$

where all pressures were measured in *mmHg*.

Left ventricular systolic pressure was derived from the calculated central systolic pressure. Previously, a pressure difference of around 5 mmHg was found between peak left ventricular systolic pressure and central systolic pressure, using catheterization.[7] The ejection times were derived from Doppler-flow imaging under B-mode.

The aortic valve geometry simulated is presented in Figure 2 and dimensions are provided in Table 1. Briefly, dimensions were obtained with respect to the T-wave of the electrocardiogram (ECG) (maximum opening area), with diameters of the aortic valve annulus and the sinus valsalva measured at the peak T-wave time, using a resting parasternal long-axis view. The two cusps were considered to be isotropic, homogenous and to have a linear stress-strain relationship. This assumption has been used in other heart valve models.[9,10,13,28] Blood was assumed to be an incompressible and Newtonian fluid.[19] All material properties are provided in Table 2 and were obtained from the literature.[29,30]

For fluid boundaries (Figure 2), pressure was applied at the inflow boundary of the aortic root at the left ventricular side. A moving ALE mesh was used, which enabled the deformation of the fluid mesh to be tracked without the need for re-meshing.[28] Second order Lagrangian elements were used to define the mesh. The mesh contained a total of 7001 elements (Figures 3a, 3b and 3c). The finite element analysis package Comsol Multi-physics (v4.2, Comsol Ltd, Cambridgeshire, UK) was used to solve the FSI model under time-dependent conditions.[9,10,11,31]

Analysis of fluid dynamics

Our studies on fluid dynamics and the effects of exercise have included an analysis of the vorticity, shear rate and cell Reynolds number. Vorticity, $\vec{\omega}$ [32] is defined as the curl of fluid velocity $\vec{u}$ according to equation (3):

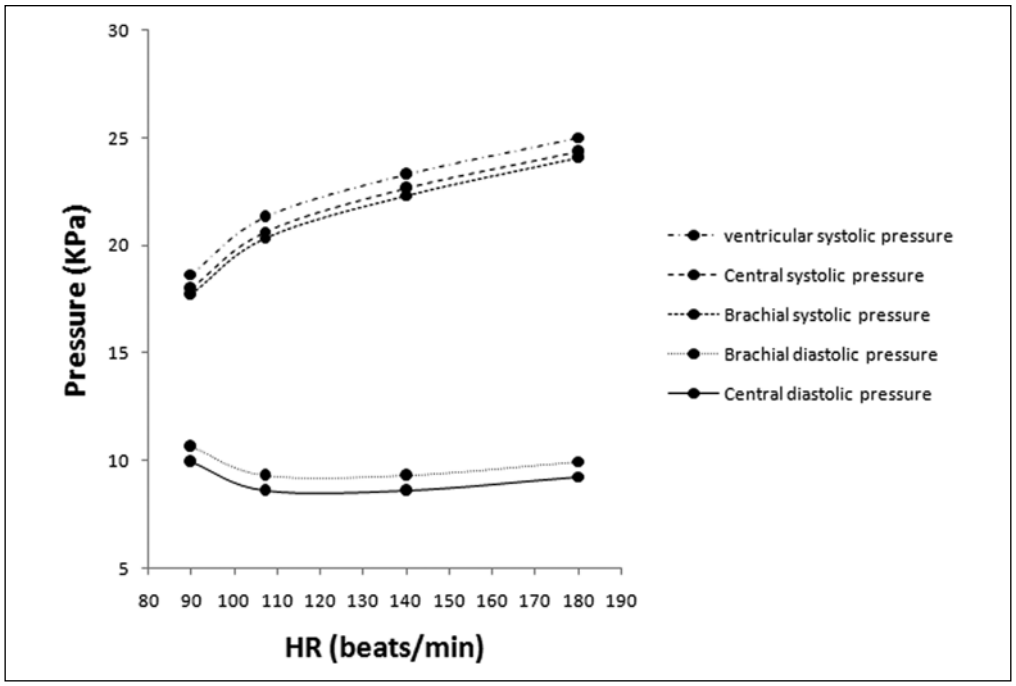

Figure 1. Interpolated curves for brachial, central and ventricular pressures.

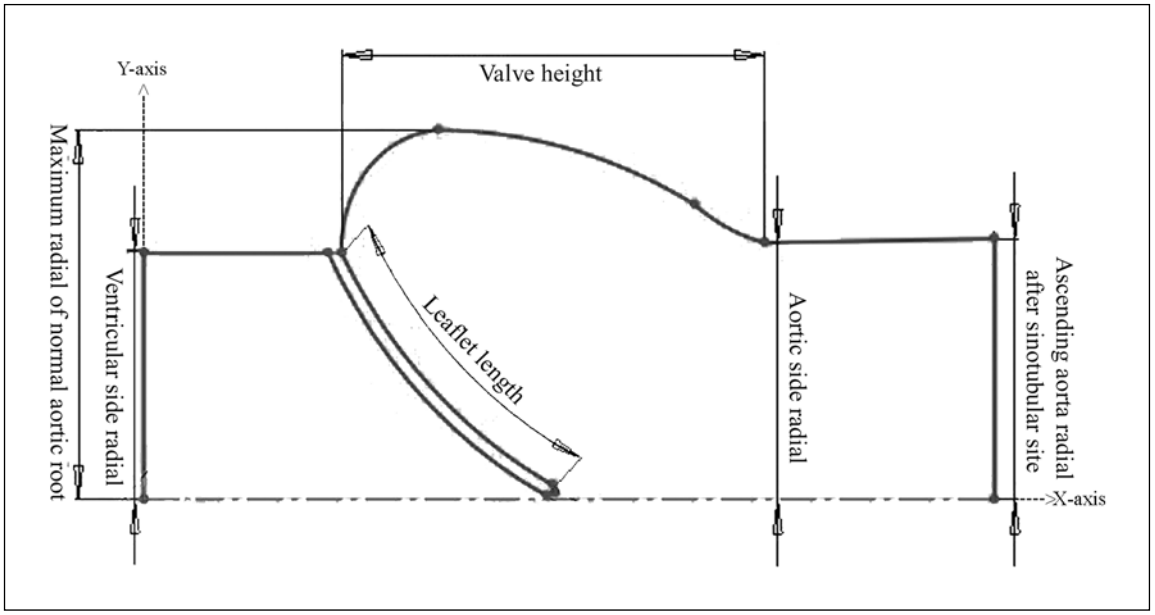

Figure 2. The geometry of the model.

$$\vec{\omega} = \nabla \times \vec{u} \tag{3}$$

Considering our two-dimensional model, equation (3) can be simplified to equation (4).

$$\vec{\omega} = \left(\frac{\partial \mathrm{v}}{\partial \mathrm{x}} - \frac{\partial \mathrm{u}}{\partial y} \right) * \vec{\mathrm{k}} \tag{4}$$

where $\boldsymbol{u}$ and $\boldsymbol{v}$ refer to the x- and y-axes velocities, respectively. Note, the x- and y-axes define two orthogonal axes of a Cartesian coordinate system, where the former is parallel to inflow and outflow boundaries of the aorta and the latter is perpendicular to these (Figure 2) and $\vec{K}$ is the unit vector along the z-axis.

Shear rate is the rate at which shear is applied (i.e. velocity gradient[33]). Shear rate $\dot{\gamma}$ is defined by equation (5).

Table 1. Geometric data of the aortic valve.

Maximum diameter of normal aortic root (mm)	Ventricular side diameter (mm)	Aortic side diameter (mm)	Ascending aorta diameter after sinotubular junction (mm)	Leaflet length (mm)	Valve height (mm)
33.3	22.2	23	23.5	16.6	20.36

Table 2. Mechanical properties of blood and aortic valve leaflets.

Viscosity (Pa.s)	Density (kg/m^3)	Young's modulus (N/m^2)	Poisson ratio
3.5 x 10^{-3}	1056	6.885 x 10^6	0.4999

$$\dot{\gamma} = \frac{\partial v}{\partial x} + \frac{\partial u}{\partial y} \quad (5)$$

The cell Reynolds number determines the stability of fluid motion within each mesh element.[32] The cell Reynolds number (Re^c) was determined using equation (6).

$$Re^c = \frac{\rho u l h}{2\mu} \gg 1 \quad (6)$$

Here h is the local mesh element size and the magnitude of the velocity vector is $\mathbf{u}$; ρ is the density and μ the viscosity of the fluid.[34]

Results

Timing

Figure 4 shows: (a) the time at which ejection started, (b) the time at which full valve opening occurred, (c) the time at which closing started and (d) the time at which closure contact occurred. The interval between (a) and (b) above is the initial opening phase, while the interval between (b) and (c) is the full-opening phase. The interval between (c) and (d) is the closing phase.

The duration of the initial opening phase, the full-opening phase and the closing phase, which decreased with increased heart rate with increasing exercise, are provided in Table 3 and Figure 5a. The duration of the initial opening phase decreased by 26% with increasing heart rate (from 98 to 169 beats per minute (bpm)). The duration of the full-opening phase decreased by 11%, whereas the duration of the closing phase decreased by 42%. The duration of the full-opening phase varied less than other time periods.

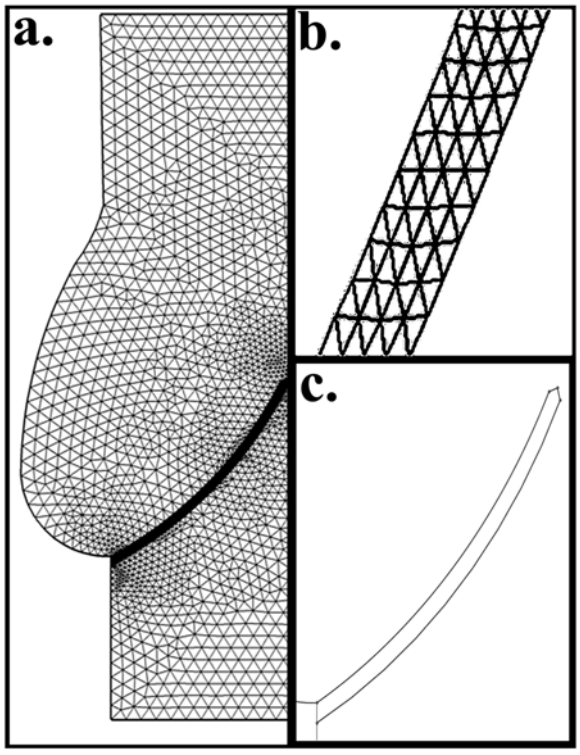

Figure 3. Mesh for (a) the fluid domain mesh generation valve cusps and (b) elements on a cusp of the solid domain mesh generation; (c) valve cusps shape.

Hemodynamics

Peak blood velocity through the aortic valve increased with exercise (Table 3 and Figure 5b). Peak velocity occurred at the time at which closure contact occurred and increased with heart rate by 19.1% (from 98 to 169 bpm). Peak velocity increased from 4.24 m.s^{-1} to 5.05 m.s^{-1}. It was located at the centre point between the leaflet tips at each heart rate. Peak blood velocity had similar correlations to heart rate (r = 0.687), cardiac output (r = 0.640) and stroke volume (r = –0.670) (Table 4).

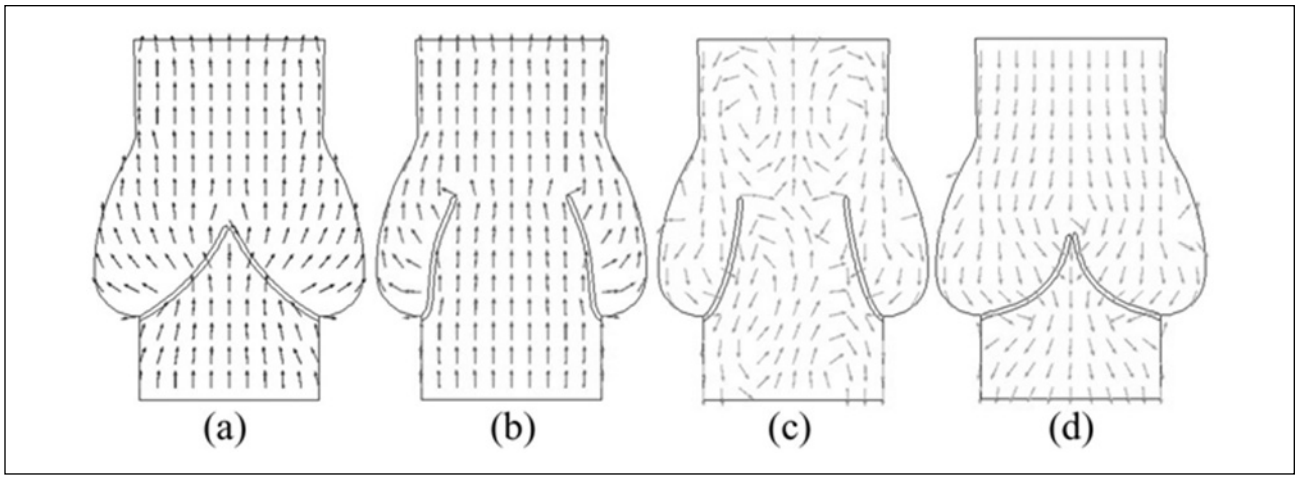

Figure 4. Ejection period's divisions: (a) the moment of ejection start, (b) the moment of reaching the major orifice region, (c) the moment of beginning of closing and (d) the moment of closure contact. Note that vectors show fluid velocity.

Table 3. Change in aortic valve leaflet deflection and associated blood velocity with exercise. Note, HR refers to heart rate.

HR	Times durations (s)			Tip Velocity (m/s)		Blood velocity peak (m/s)	
	The initial opening phase	Full-opening phase	Closing phase	During full valve opening phase	During closure contact phase	Full-opening phase	During closure contact phase
98	0.042	0.141	0.078	0.46	0.83	3.25	4.24
106	0.039	0.14	0.07	0.45	0.96	3.43	3.81
114	0.035	0.141	0.062	0.38	1.00	3.60	3.78
125	0.034	0.139	0.059	0.39	1.01	3.66	3.84
136	0.033	0.134	0.055	0.41	1.15	3.73	5.47
147	0.033	0.131	0.053	0.42	1.14	3.78	4.49
153	0.035	0.128	0.05	0.50	1.12	3.80	5.82
159	0.031	0.13	0.046	0.43	1.23	3.83	4.79
169	0.031	0.125	0.045	0.44	1.23	3.88	5.05
Total increment (%)	–26	–11	–42	–4.35	43.6	19.3	19.1

Peak vorticity during the full-opening phase increased with heart rate (Table 5 and Figure 5c). It increased by 14.8%, from 17594 s^{-1} (98 bpm) to 20190 s^{-1} (169 bpm). Peak vorticity during full valve opening also increased overall with exercise (increasing by 43.6%). However, the peak vorticity during the closing phase did not change with exercise (remaining approximately constant, with values around 5565 s^{-1}; Table5 and Figure 5c). Peak vorticity was consistently located at the leaflet tip throughout exercise. Peak vorticity correlated to cardiac output (r = 0.978) and heart rate (r = 0.936) better than stroke volume (r = –0.382) (Table 4).

Note, COD refers to cardiac output by Doppler, SVD refers to stroke volume by Doppler and HR refers to heart rate.

The peak shear rate during the full-opening phase increased with heart rate, but not during the closing phase (with values of around 17921 s^{-1}; Table 5 and Figure 5d). The peak of the shear rate increased by 15.8%, from 46541 s^{-1} (98 bpm) to 55277 s^{-1} (169 bpm). The peak shear rate during full valve opening increased by 25.6% from a heart rate of 98 bpm to 169 bpm. The peak shear rate during the ejection phase was located at the leaflet tip throughout the exercise. Peak shear rate correlated to cardiac output (r = 0.973) and heart rate (r = 0.928) better than stroke volume (r = –0.360) (Table 4).

The peak cell Reynolds number increased by 20% from a heart rate of 98 bpm (215) to a heart rate of 169 bpm (258; Table 5 and Figure 5e). The peak cell Reynolds number for all heart rates was located along the length of the aortic root close to the valve leaflets. Peak cell Reynolds number correlated to cardiac output (r = 0.977) and heart rate (r = 0.936) better than stroke volume (r = –0.377) (Table 4).

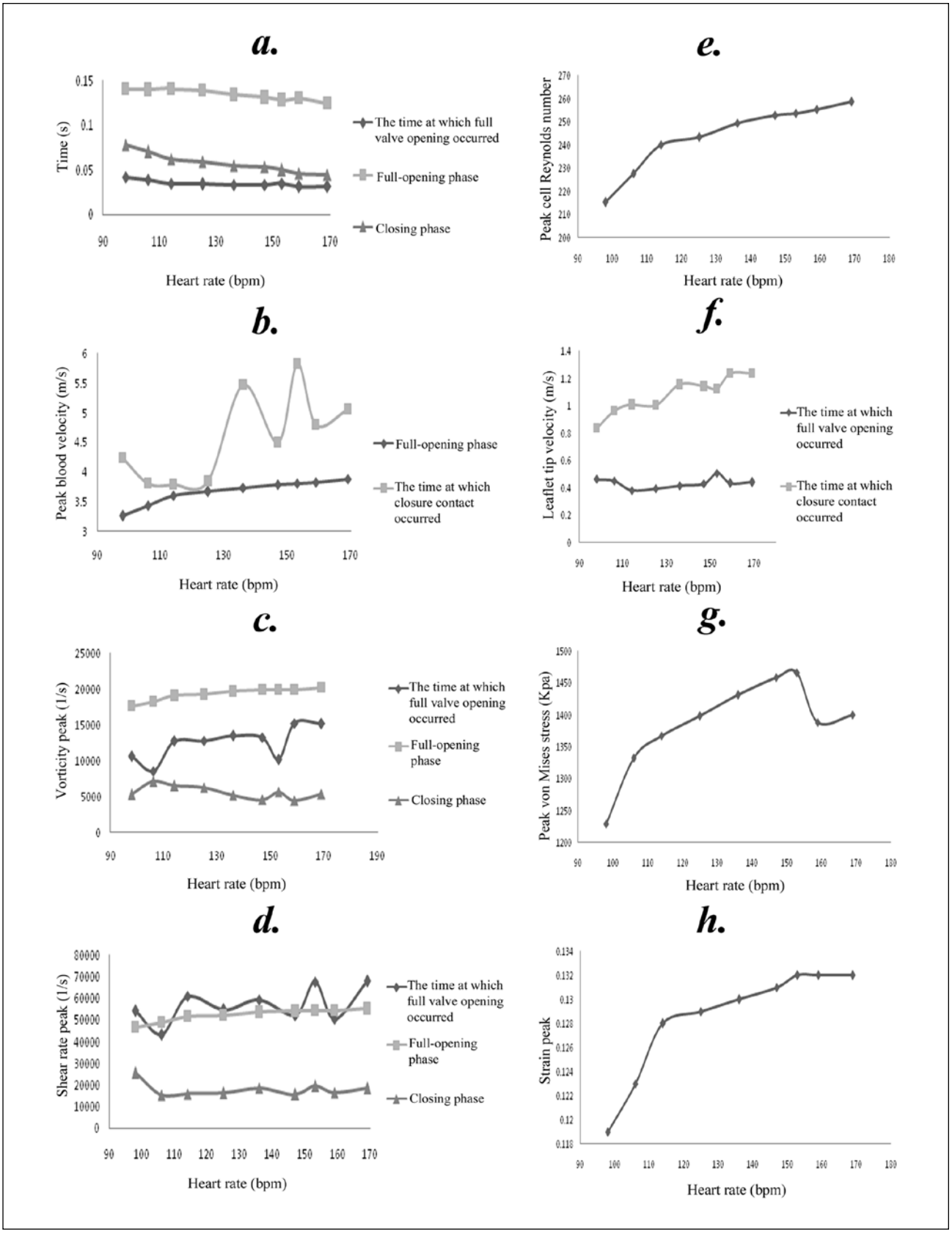

Figure 5. Changes in: (a) Time, (b) Peak blood velocity, (c) Vorticity peak, (d) Shear rate peak, (e) Peak cell Reynolds number, (f) Leaflet tip velocity, (g) Peak von Mises stress and (h) Strain peak with heart rate.

Leaflet mechanics

The leaflet tip velocity (0.44 $m.s^{-1}$) during full valve opening did not change much with exercise (Table 3 and Figure 5f). However, the leaflet tip velocity during the closing phase increased with heart rate, increasing from 0.83 $m.s^{-1}$ (at 98 bpm) to 1.23 $m.s^{-1}$ (at 169 bpm). This velocity correlated to cardiac output (r = 0.960) better than heart rate (r = 0.949) or stroke volume (r = 0.420) (Table 4-).

Peak von Mises stress and strain tensor increased with increasing heart rate (Table 6 and Figures 5g & 5h). However, at heart rates above 153 bpm, there was a decrease in von Mises stress. The highest von Mises stress (1.466 MPa) was predicted at 153 bpm. Peak stresses and strains were located at the aortic root at all levels of exercise. The von Mises stress peak correlated to cardiac output (r = 0.807) better than heart rate (r = 0.729) or stroke volume (r = –0.113) (Table 4). The strain peak correlated to cardiac output (r = 0.951) better than heart rate (r = 0.897) or stroke volume (r = -0.298) (Table 4).

Discussion

Study finding

This study investigated the hemodynamic flows through a two-dimensional FSI model of natural aortic heart valve and their variation with exercise during systole. To our knowledge, this is the first time that an FSI model has been integrated with exercise measurements to enable numerical predictions of hemodynamics such as vorticity, cell Reynolds number and shear rate. The aortic valve FSI model was subject specific in that its dimensions and boundary conditions were based on measurements made from a single individual. Different boundary conditions were applied to the model according to the heart rate and blood pressure measured under different intensity of exercise. The main findings from this study are that, with increasing exercise (i.e. increasing heart rate/blood pressure) during the left ventricular systole phase, the:

- vorticity increased with exercise and peaked during full valve opening at 20190 s^{-1};
- shear rate increased with exercise and peaked during closure contact at 19469 s^{-1};
- leaflet tip velocity increased with exercise, peaking during closure contact with a velocity of 1.23 $m.s^{-1}$;
- cell Reynolds number increased with exercise up to 258;
- peak blood flow velocity through the orifice region increased with exercise up to 5.82 $m.s^{-1}$, peaking during closure contact;
- von Mises stress increased with exercise, peaking at 1.466 MPa;
- strain increased with exercise, peaking at 0.132.

Previously, this model was validated by comparison with echo-Doppler results in terms of cardiac output and stroke volume.[26] The current study demonstrates the feasibility of obtaining a range of time-dependent and variable boundary conditions (e.g. altered due to exercise) and using these to predict cardiovascular performance.

Clinical application and reliability

Predictions for mean velocity, cardiac output and stroke volume were previously validated against subject specific measurements using Doppler-echocardiography (ECG).[26] Model predictions never differed by more than around 15% of the clinical measurement. Our previous study focused on validating the model against measures of cardiac function that could be reliably measured using clinical procedures, with varying exercise.

Our current findings demonstrate that vorticity, shear rate and cell Reynolds number are strongly correlated to cardiac output and heart rate, but not to stroke volume. These findings are of potential future value to two distinct treatment strategies for cardiovascular disease: transplant and artificial heart valve development. Such a tool holds potential for clinical applications, given the current limitations associated with existing invasive and non-invasive techniques. These were discussed previously.[26] Briefly, invasive methods (e.g. catheterization-thermodilution) pose risks to the patient and clinical staff, whereas non-invasive methods (e.g. echo-Doppler) have low repeatability (±11%).[35] However, the application of modeling to the treatment strategies will require future model development. Our current results demonstrate the feasibility of using computational models to identify fluid flow parameters altered by cardiac function, albeit under physiological conditions.

Comparison to the literature

Following a literature search, we have not found a previous comparable study that combined a clinical and numerical approach to predict aortic valve hemodynamics during exercise. We have used brachial systolic and diastolic pressures as a boundary condition, but have not neglected valvular-vascular pressure differences between the left ventricle and brachial measurements.[26] We found, previously, that our predictions on cardiac output and stroke volume compared well to other numerical studies that predicted cardiac output at rest.[16,26,36,37]

Our current results also agree with the literature available for comparison. For example, our model

Table 4. Linear correlations between predicted parameters (valve mechanics and blood-flow dynamics) and cardiac output (COD), stroke volume (SVD) and heart rate (HR). Note equations where of the form $y = aX + b$.

Y	X	a	b	R^2	r
Vortex peak (s^{-1})	COD (ml/min)	0.338	14002	0.957	0.978
Vortex peak (s^{-1})	SVD (ml/beat)	79.71	28636	0.146	–0.382
Vortex peak (s^{-1})	HR (bpm)	32.93	14877	0.877	0.936
Shear rate peak (s^{-1})	COD (ml/min)	1.128	34689	0.947	0.973
Shear rate peak (s^{-1})	SVD (ml/beat)	251.6	81837	0.129	–0.360
Shear rate peak (s^{-1})	HR (bpm)	109.4	37665	0.862	0.928
Reynolds number	COD (ml/min)	0.005	157.1	0.956	0.977
Reynolds number	SVD (ml/beat)	–1.285	394.2	0.142	–0.377
Reynolds number	HR (bpm)	0.537	171.4	0.876	0.936
Blood velocity peak ($m.s^{-1}$)	COD (ml/min)	1.90E-04	1.620	0.410	0.640
Blood velocity peak ($m.s^{-1}$)	SVD (ml/beat)	–0.119	18.62	0.449	–0.670
Blood velocity peak ($m.s^{-1}$)	HR (bpm)	0.020	1.813	0.472	0.687
Tip Velocity peak ($m.s^{-1}$)	COD (ml/min)	5E-05	0.285	0.922	0.960
Tip Velocity peak ($m.s^{-1}$)	SVD (ml/beat)	–0.016	3.05	0.280	0.420
Tip Velocity peak ($m.s^{-1}$)	HR (bpm)	0.005	0.394	0.902	0.949
Peak von Mises (kPa)	COD (ml/min)	0.023	1024	0.650	0.807
Peak von Mises (kPa)	SVD (ml/beat)	–1.946	1613	0.012	–0.113
Peak von Mises (kPa)	HR (bpm)	2.124	1100	0.532	0.729
Peak strain	COD (ml/min)	2E-06	0.101	0.904	0.951
Peak strain	SVD (ml/beat)	–3.24E-04	+ 0.166	0.089	–0.298
Peak strain	HR (bpm)	1.65E-04	0.106	0.805	0.897

predicted the viscous forces in the aortic valve area created a large vortex, trapped in the sinus cavity. That observation is in agreement with established results in the literature.[38–40] In our study, the peak vorticity at different heart rate stages varied from 4449 s^{-1} to 20190 s^{-1} throughout the protocol. We have not been able to find experimental measurements for biological heart valves to compare with these predictions. However, for mechanical heart valves, vorticity has been reported in the range of 5700 s^{-1} to 42600 s^{-1}, typically measured at rest.[41] Our results are comparable to this range, apart from the higher values reported for mechanical valves. This is possibly because our study modeled a natural valve. Mechanical valves would be anticipated to have greater peak vorticity due to their opening/closuring mechanisms. Mechanical valves, for example, lead to blood hemolysis and rupturing of red blood cells.[42] Lower vorticity is, thus, anticipated as being reasonable for a biological valve.

Our predicted peak velocity occurred during valve closure and varied from 3.8 $m.s^{-1}$ to 5.8 $m.s^{-1}$ (increasing with exercise). This was compared to the values ranging from 0.75 $m.s^{-1}$ to 4.00 $m.s^{-1}$ found in the literature under rest conditions.[6,13-15,40] It should be noted that all our measurements were under exercise conditions and, therefore, it is not surprising that our values for peak velocity exceed those measured at rest. Furthermore, values in the literature arise from a variety of subjects of different ages (e.g. infants and elders) at rest. Our lowest peak velocity of 3.8 $m.s^{-1}$ was obtained at a heart rate of 98 bpm. Thus, the higher predicted velocity is reasonable when compared to other studies.[42]

Peak von Mises stress in our study ranged from 1229 kPa to 1466 kPa. This compares well to values in the range of 60 kPa[4] to 1700 KPa[43] available in the literature. Our peak strains ranged from 0.119 to 0.132 during exercise. These values are in general agreement with predicted peak strains in the region on 0.12 in the literature [37].

In our model, we have made subject specific predictions; it is not anticipated that our values should precisely match other predictions. For example, De Hart et al.[15] applied time-dependent plug flow velocity at the upstream boundary of the aortic root and time-dependent pressure waveform at the downstream boundary. In our model, the applied boundary conditions were derived following clinical measurement.

In our current study, we have found shear stress to increase with exercise (from 64 to 238 Pa). Although we have not been able to find comparable values in the literature, these are lower than shear stresses reported for mechanical heart valves.[44] used for aortic valve replacement (200 and 800 Pa). This is expected as the closure of mechanical valves is known to induce high shear stress.[45]

Local cell Reynolds number increased from 215 to 259 with exercise.[35] These values are lower than the peak values of 4000 measured *in vivo*.[46] However, we have determined the cell Reynolds number, not the Reynolds

Table 5. Change in predicted hemodynamics with exercise. Note, COD refers to cardiac output by Doppler, SVD refers to stroke volume by Doppler and HR refers to heart rate. Cell Reynolds number as measured during the ejection period.

HR	Vortex (s^{-1})			Shear rate (s^{-1})			Reynolds number	SVD (ml/beat)	COD (ml/min)
	During full valve opening phase	During full-opening phase	During closure contact phase	During full valve opening phase	During full-opening phase	during closure contact phase			
98	10540	17594	5232	54048	46541	25418	215	115.8	11356
106	8509	18221	7075	43134	48759	15433	227	119.4	12651
114	12695	19056	6488	60861	51766	16007	240	123.3	14051
125	12781	19247	6235	54695	52284	16150	243	122.4	15298
136	13474	19670	5149	59476	53493	18631	249	118.9	16172
147	13265	19856	4528	52267	54203	15542	252	117.2	17225
153	10131	19901	5620	67692	54364	19469	253	113.3	17330
159	15225	19914	4449	50539	54444	16278	255	112.8	17941
169	15135	20190	5303	67892	55277	18359	258	111.5	18849
Total increment (%)	43.6	14.8	1.6	25.6	18.8	27.8	20	–3.7	66

Table 6. Variations of maximum von Mises stress and strain with heart rate during exercise.

Heart rate (beats/min)	Peak von Mises (KPa)	Peak strain
98	1229	0.119
106	1333	0.123
114	1367	0.128
125	1398	0.129
136	1431	0.130
147	1459	0.131
153	1466	0.132
159	1388	0.132
169	1400	0.132
Total increment (%)	13.9	10.1

number. This provides the peak Reynolds number calculated in an individual mesh element. Therefore, while the predicted value is representative of the Reynolds number, it is not equivalent. Our cell Reynolds number increased with exercise, therefore, our results qualitatively show that the Reynolds number increases with exercise.

Limitations and future trends

An in-depth discussion of the limitations of the FSI model has been provided previously.[26] Briefly, the main limitations are that:

- A constant orifice area and a single diameter for the ascending aorta were used, along with simplifications of the mechanical leaflet properties, in the model;
- Clinical assessment of hemodynamics is reached on the basis of statistical/generalised information. However, variation in mechanical properties of natural aortic heart valves has been reported[47] and its effect on numerical predictions assessed for a 2D heart valve model.[26] Cardiac output varied by approximately 5% over the reported range of mechanical properties.
- A two-dimensional model was used to investigate a three-dimensional structure. The model predictions may improve by the use of a 3D model.[48] This increase in precision, however, has to be balanced against the short solution time for a 2D FSI model. Our model solution time was as low as 15 min, which has potential for translation into clinical practice.
- Blood was considered to be an incompressible, Newtonian fluid. This may affect specific hemodynamic predictions, but it is not expected to alter the conclusions from our study. This is because we have focused on hemodynamic trends with exercise. Regardless, for large scale flow in

the cardiovascular system, blood properties approximate that of a Newtonian fluid.[19]

- Only one subject was assessed in our study. Numerical simulation, however, needs specific values, such as boundary conditions and geometric dimensions as well as mechanical properties. There is also a current trend towards subject-specific modeling (e.g., Van Steenhoven et al.[49]), with the potential benefit of individualised healthcare predictions in future. However, before our model is translated into clinical practice, a larger clinical trial with more subjects would be necessary.

Despite model limitations, we previously demonstrated good agreement with clinical measurements and the general literature.[26] Further developments could include the use of a range of values for statistical comparison by including variability in the models.[10]

Conclusion

A subject-specific, two-dimensional, fluid-structure, interaction model of the aortic valve has been used to make hemodynamic predictions at rest and during exercise. Our model predicted that vortex, shear rate, peak velocity and Reynolds number increase with increasing levels of exercise. The stresses induced in the aortic valve leaflets also increased with exercise. These increases correlated to the increased heart rate and cardiac output, but not the stroke volume. However, further appropriate clinical studies and trials are necessary to develop the computational model towards translation into clinical practice.

Declaration of conflicting interest

The authors declare that there is no conflict of interest.

Funding

During the study, DME was supported by a Marie Curie Intra-European Fellowship within the 7th European Community Framework Programme (Programme number: FP7/2007-2013; under grant agreement n°252278).

References

1. Murphy SL, Xu J. Deaths: preliminary data for 2010. *National Vital Statistics Reports* 2012; 4: 31.
2. Grunkemeier GL, Li HH, Starr A. Heart valve replacement: a statistical review of 35 years results—Discussion. *J Heart Valve Dis* 1999; 8: 470–471.
3. Butchart EG, Ionescu A, Payne N, Giddings J, Grunkemeier GL, Fraser AG. A new scoring system to determine thromboembolic risk after heart valve replacement. *Circulation* 2003; 108: 68–74.
4. Martin UJ, Diaz-Abad M, Krachman SL. Hemodynamic monitoring. In:Criner GJ, Barnette RE, Alonzo GE (eds). *Critical care study guide: text and review*. 2nd Ed. 2010, Springer-Verlag, New York, LLC. Pp 51–78.
5. Giddens DP, Yoganathan AP, Schoen FJ. Prosthetic cardiac valves. *Cardiovasc Pathol* 1993; 2 (Suppl): 167–177.
6. Piérard LA, Lancellotti P. Stress testing in valve disease. *Heart* 2007; 93: 766–772.
7. Laske A, Jenni R, Maloigne M, Vassalli G, Bertel O, Turina MI. Pressure gradients across bileaflet aortic valves by direct measurement and echocardiography. *Ann Thorac Surg* 1996; 61:48–57.
8. Al-Atabi M, Espino DM, Hukins DWL. Computer and experimental modeling of blood flow through the mitral valve of the heart. *J Biomech Sci Eng* 2010; 5: 78–84.
9. Espino DM, Shepherd DE, Hukins DW. Evaluation of a transient, simultaneous, Arbitrary Lagrange Euler based multi-physics method for simulating the mitral heart valve. *Comput Methods Biomech Biomed Engin* 2013; Epub DOI: 10.1080/10255842.2012.688818
10. Espino DM, Shepherd DE, Hukins DW. Development of a transient large strain contact method for biological heart valve simulations. *Comput Methods Biomech Biomed Engin* 2013; 16: 413–424.
11. Espino DM, Shepherd DE, Hukins DW. A simple method for defining contact modeling within multi-physics software. *J Mech* 2013; 29: N9-N14.
12. Winslow AM. Numerical solution of the quasilinear Poisson equation in a nonuniform triangle mesh. *J Comput Phys* 1966; 1:149–172.
13. De Hart J, Peters GW, Schruers PJ, Baaijens FP. A two-dimensional fluid-structure interaction model of the aortic valve. *J Biomech* 2000; 33:1079–1088.
14. De Hart J, Peters GW, Schreurs PJ, Baaijens FP. A three-dimensional computational analysis of fluid–structure interaction in the aortic valve. *J Biomech* 2003; 36: 103–112.
15. De Hart J, Baaijens FP, Peters GW, Schreurs PJ. A computational fluid-structure interaction analysis of a fiber-reinforced stentless aortic valve. *J Biomech* 2003; 36: 699–712.
16. Griffith BE, Peskin CS. On the order of accuracy of the immersed boundary method: higher order convergence rates for sufficiently smooth problems. *J Comput Phys* 2005; 208: 75–105.
17. Griffith BE, Hornung RD, McQueen DM, Peskin CS. An adaptive, formally second order accurate version of the immersed boundary method. *J Comput Phys* 2007; 223: 10–49.
18. Griffith BE, Luo XY, McQueen DM, Peskin CS. Simulating the fluid dynamics of natural and prosthetic heart valves using the immersed boundary method. *Int J Appl Mech* 2009; 1: 137–177.
19. Caro CG, Pedley TJ, Schroter RC, Seed WA. *The mechanics of the circulation*. Oxford: Oxford University Press 1978.
20. Bellhouse BJ. The fluid mechanics of heart valves. In: DH Bergel (ed). *Cardiovascular fluid dynamics*. Volume 1. London, Academic Press 1972.

21. Donea J, Giuliani S, Halleux JP. An arbitrary Lagrangian–Eulerian finite element method for transient dynamic fluid–structure interactions. *Comput Methods Appl Mech Engrg* 1982; 33: 689–723.
22. Dowell EH, Hall KC. Modeling of fluid-structure interaction. *Annu Rev Fluid Mech* 2001; 33: 445–490.
23. Van de Vosse FN, De Hart J, Van Oijen CHGA, et al. Finite-element-based computational methods for cardiovascular fluid-structure interaction. *J Eng Math* 2003; 47: 335–368.
24. Labrosse MR, Lobo K, Beller CJ. (2010) Structural analysis of the natural aortic valve in dynamics: from unpressurized to physiologically loaded. *J Biomech* 2010; 43: 1916–1922.
25. Nobili M, Sheriff J, Morbiducci U, Redaelli A, Bluestein D. Platelet activation due to hemodynamic shear stresses: damage accumulation model and comparison to in vitro measurements. *ASAIO J* 2008; 54: 64–72.
26. Bahraseman HG, Hassani K, Navidbakhsh M, Espino DM, Sani ZA, Fatouraee N. Effect of exercise on blood flow through the aortic valve: a combined clinical and numerical study. *Comput Methods Biomech Biomed Engin* 2014; 17: 1821–1834.
27. Park SH, Lee SJ, Kim JY, et al. Direct comparison between brachial pressure obtained by oscillometric method and central pressure using invasive method. *Soonchunhyang Med Sci* 2011; 17: 65–71.
28. Weinberg EJ, Kaazempur-Mofrad MR. (2008) A multiscale computational comparison of the bicuspid and tricuspid aortic valves in relation to calcific aortic stenosis. *J Biomech* 2008 41: 3482–3487.
29. Govindarajan V, Udaykumar HS, Herbertson LH, Deutsch S, Manning KB, Chandran KB. Two-dimensional FSI simulation of closing dynamics of a tilting disk mechanical heart valve. *J Med Devices* 2010; 4: 011001(1–11).
30. Koch TM, Reddy BD, Zilla P, Franz T. Aortic valve leaflet mechanical properties facilitate diastolic valve function. *Comput Methods Biomech Biomed Engin* 2010 13: 225–234.
31. Formaggia L, Nobile F. A stability analysis for the arbitrary Lagrangian Eulerian formulation with finite elements. *East–West J Numer Math* 1999; 7: 105–132.
32. Kheradvar A, Pedrizzetti G. *Vortex formation in the cardiovascular system*. Springer, London, Dordrecht, Heidelberg, New York. 2012, pp 45–73.
33. Hochareon P, Manning KB, Fontaine AA, Tarbell JM, Deutsch S. Wall shear-rate estimation within the 50 cc Penn State artificial heart using particle image velocimetry. *J Biomech Eng* 2004; 126: 430–437.
34. Comsol Users Manual. *Comsol multiphysics users guide*. Comsol Ltd., London, 2011.
35. Maylab Users Manual. *Maylab advanced operation*. Biosound Esaote Inc., New York. 2008
36. Guyton AC, Hall JE. Overview of circulation; medical physics of pressure. *Textbook of Medical Physiology* 9th ed. WB Saunders, Philadelphia, Pennsylvania, 1996.
37. Murgo JP, Westerhof N, Giolma JP, Altobelli SA. Aortic input impedance in normal man: relationship to pressure wave forms. *Circulation* 1980; 62: 105–116.
38. Peskin CS, Wolfe AW. The aortic sinus vortex. *Fed Proc* 1978; 37: 2784–2792.
39. Peskin CS. The fluid dynamics of heart valves: experimental, theoretical, and computational methods. *Annu Rev Fluid Mech* 1982; 14: 235–259.
40. Van Steenhoven AA, Van Dongen MEH. Model studies of the closing behaviour of the aortic valve. *J Fluid Mech Digit Arch* 1979; 90: 21–32.
41. Krishnan S, Udaykumar HS, Marshall JS, Chandran KB. Two-dimensional dynamic simulation of platelet activation during mechanical heart valve closure. *Ann Biomed Eng* 2006; 34: 1519–1534.
42. Bonow RO, Mann DL, Zipes DP, Libby P. Braunwald's heart disease: a textbook of cardiovascular medicine. 9th ed. Philadelphia, PA, Saunders 2011.
43. Hsu CH, Nguyen BS, Vu HH, Hemodynamics and mechanical behavior of aortic heart valves: a numerical evaluation. *4th International Conference on Biomedical Engineering and Informatics, BMEI 2011*, Shanghai, China, 2011.
44. Yoganathan AP, Chandran KB, Sotiropoulos F. (2005) Flow in prosthetic heart valves: state-of-the-art and future directions. *Ann Biomed Eng* 2005; 33: 1689–1694.
45. Espino DM. Polymers as replacement materials for heart valves and arteries. In: Jenkins M, ed. *Biomedical polymers*. Woodhead Publishing Ltd., Cambridge. 2007, pp 111–140.
46. Nerem RM, Seed WA. An in vivo study of aortic flow disturbances. *Cardiovasc Res* 1972; 6: 1–14.
47. Kortsmit J. Non-invasive assessment of leaflet deformation and mechanical properties in heart valve tissue engineering [dissertation]. [Eindhoven]: *Technische Universiteit Eindhoven* 2009
48. Bahraseman GH, Hassani K, Khosravi A, et al. Estimation of maximum intraventricular pressure: a three-dimensional fluid–structure interaction model. *Biomedical Engineering Online* 2013; 12: 122. DOI:10.1186/1475–925X-12–122.
49. Öhman C, Espino DM, Heinmann T, Baleani M, Delingette H, Viceconti M (2011) Subject-specific knee joint model: design of an experiment to validate a multi-body finite element model. *Visual Comp* 2011; 27: 153–159.